2C1-5

Numerical Estimations of the Propagation Characteristics of Wireless Links in High-Speed Train Cars

#Takashi Hikage [1], Masami Shirafune [1], Toshio Nojima [1],
Wataru Yamada [2], Takatoshi Sugiyama [2]
[1] Graduate School of Information Science and Technology, Hokkaido University
Kita 14, Nishi 9, Kita-ku, Sapporo, 060-0814 Japan
{hikage, shirafune, nojima}@wtemc.ist.hokudai.ac.jp
[2] NTT Access Network Service Systems Laboratories, NTT Corporation
1-1 Hikari-no-oka, Yokosuka-Shi, Kanagawa, 239-0847 Japan
{yamada.wataru, sugiyama.takatoshi}@lab.ntt.co.jp

1. Introduction

Demand for wireless broadband access services in long-distance transportations continues to grow. Several railway companies have recently begun in-car wireless LAN services [1]. In order to advance the radio link design in support of such services, an accurate and reliable method for estimating the electromagnetic environment in actual situations is required. However, comprehensive on-site field measurements cost too much, and it is difficult to carry them out precisely. In addition, measurements must take account of the absorbing effects due to many passengers triggering the drawbacks of poor feasibility and repeatability. This study introduces an accurate and reliable method of estimating electromagnetic field (EMF) distributions in train cars so as to advance the radio link design of wireless LANs operated inside train cars. The authors previously proposed an EMF estimation method for a typical commuter train based on FDTD analysis and parallel computing [2]. This paper evaluates the propagation characteristics in a High-Speed Train Car (HSTC). Using newly developed numerical models of HSTC, which include many passengers, EMF distributions created by a 5.2 GHz wireless transmitter inside the HSTC are analyzed and propagation characteristics are evaluated. In order to estimate the effect of the absorption by the passengers' bodies, simplified histograms of the electric field distributions throughout the whole interior of the car are derived.

2. High-speed train car model and estimation method

Fig. 1 shows the two-car HSTC model with passengers used in this study. The model configurations, such as body dimensions and seat arrangements are based on an actual HSTC now in active service [3]. A 5.2 GHz wireless LAN access point simulator, a vertical polarized half-wavelength dipole antenna located near the ceiling, is assumed to be placed at the centre of the first car as shown in Fig. 1. The dimensions of the train used in the analysis model are as accurate as possible. Parts external to the cars such as rails, pantographs and so on, are not modelled. The dimensions of the two cars are: overall length of 49.3 m, width of 3.2 m and height of 2.6 m. The train body is made of perfect electric conductor (P.E.C.). Also the ceiling luggage racks are made of P.E.C.. The window panels are 10 mm thick glass. The seats consist of P.E.C. and lossy material. The connecting door between the cars is modelled in the open state. Homogeneous numerical humans [4] with seated posture are used as passengers. This model is realistic dimensions and the electric parameters are taken from a 2/3 muscle-equivalent phantom [5]. In order to estimate the absorption effects by the passengers' bodies, the occupancy rate is varied from 0 % to 100 % (0 % : without passengers, 20 % : 37 passengers, 40 % : 74 passengers, 60 % : 111 passengers, 80 % : 149

passengers and full capacity : 186 passengers). Tables 1 and 2 summarize the FDTD parameters and material parameters, respectively.

3. Field estimation results

Fig. 2 shows the 2-dimensional electric field distributions obtained by the FDTD analyses for the occupancy rates of 0 and 100 %. A vertically polarized wave at 30 dBm at 5.25 GHz is radiated from a half-wavelength dipole, located in car #1. Vertical (Ey) polarized electric field distributions on the horizontal plane at the height of 0.68 m above the floor are shown in the figures. These figures show that attenuation effect due to passengers' bodies cannot be neglected when estimating the EMF in train cars. At the occupancy rate of 100 %, the electric field intensity in car #2 is, except the aisle, about 20 dB lower than the no-passenger case. Fig. 3 shows Poynting vector distributions inside the cars without passengers. From the figure, we see that wave propagation inside the cars is very complicated due to the multi-reflection environment. Additionally, the waves travelling inside the cars are dominant compared with waves that re-enter the car from the outside of the car because the door between the cars is open in this model.

Next, we apply histogram analysis to quantitatively assess of the effects of RF absorption by passengers. Based on the electric field distributions, we examined the histograms of each train car. Fig. 4 shows the histograms for both cases, without passengers and full capacity, obtained from the field distributions shown in Fig.2. Additionally, the modes of the histograms are plotted in Fig.5 with regard to occupancy rate. These are evaluated from 2-dimensional electric field distributions of the whole observation plane, 0.68 m above the floor. From the figures, we can confirm that the maximum attenuation of the electric field due the passengers is about 10 dB in car #1, which has the highest passenger density. In addition, the attenuation increases linearly with occupancy rate as shown in Fig.5. The rates of attenuation increase for car #1 and car #2 are -0.1 dB/% and -0.18 dB/%, respectively.

4. Conclusions

EMF distributions established in high-speed train cars as experienced by a 5.2 GHz wireless LAN terminal were estimated. Based on field distribution analyses, the energy absorption effects of the passengers' bodies were determined. This absorption cannot be neglected inside train cars. The proposed numerical estimation method can evaluate the degradation in quality and service availability of wireless access due to the absorption effects quantitatively and will contribute to the advancement of radio link designs for wireless LANs operating inside train cars. We intend to conduct other estimations that consider different train models, more antenna sources, and different types of transmitting antenna.

References

[1] e.g. http://www.mir.co.jp/wireless/

[2] T. Hikage, T. Nojima, W. Yamada, and T. Sugiyama,:"Propagation Characteristics of Wireless Communications in Crowded Train Cars," Proc. 2011 International Symposium on Antennas and Propagation, WeE1-2, Jeju, Korea, Oct. 2011.

[3] N. Kita, T. Ito, S. Yokoyama, M.-C. Tseng, Y. Sagawa, M. Ogasawara, and M. Nakatsugawa, "Experimental Study of Propagation Characteristics for wireless communications in High-Speed Train Cars," proc. European Conference on Antennas and Propagation 2009, pp. 897- 901, 2009.

[4] T. Nagaoka, et al., "Development of Realistic High-Resolution Whole-Body Voxel Models of Japanese Adult Male and Female of Average Height and Weight, and Application of Models to Radio-Frequency Electromagnetic-Field Dosimetry " Physics in Medicine and Biology, Vol.49, pp.1-15, 2004.

[5] C.Gabriel, Brooks Air Force Technical Report AL/OE-TR-1996-0037, 1996.

[6] Taflove, Computational Electromagnetics, Artech House, Boston, 1995.

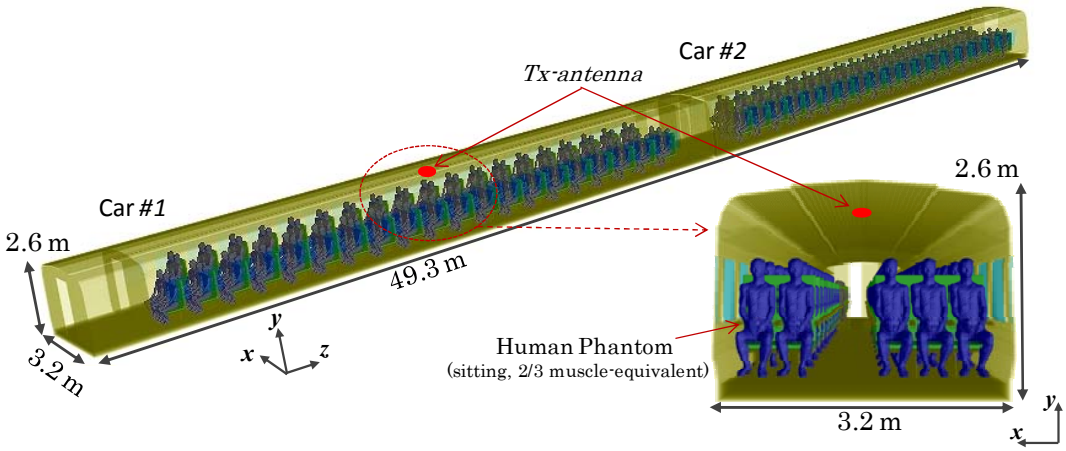

Figure 1: FDTD model for two adjacent high-speed train cars including passengers.

Table 1: FDTD parameters

Problem Space	796 × 600 × 9880 (x × y × z) cells
Cell size	△= 5 mm (cubic)
Frequency	5.25 GHz (C.W.)
Absorbing Boundary Condition	C.P.M.L. [6] (10 layers)
Iteration	7000 periods
Antenna	λ /2 dipole (Vertical polarization) Input power: 1 W
Number of computational nodes	10
Total required memory	790 GB

Table 2: Train-car materials

Media	ε_r	δ [S/m]
Body	-	∞ (P.E.C.)
Metal parts	-	∞ (P.E.C.)
Window	5.0	0.003
Pad of seat	2.0	0.001

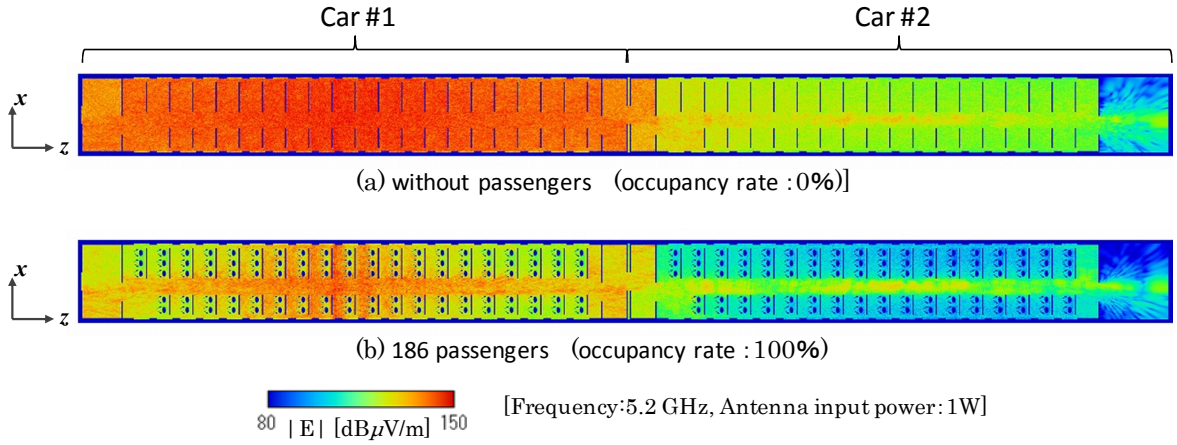

Figure 2: Electric field distributions inside the HSTC on the horizontal plane at the height of 0.68 m above the floor.

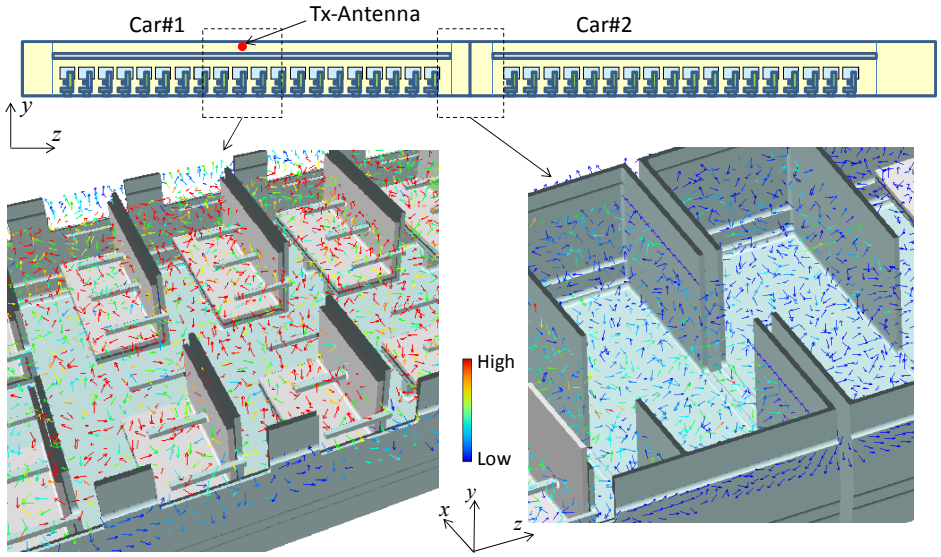

Figure 3: Poynting vector distributions inside the train cars on the horizontal plane at the height of 0.68 m above the floor.

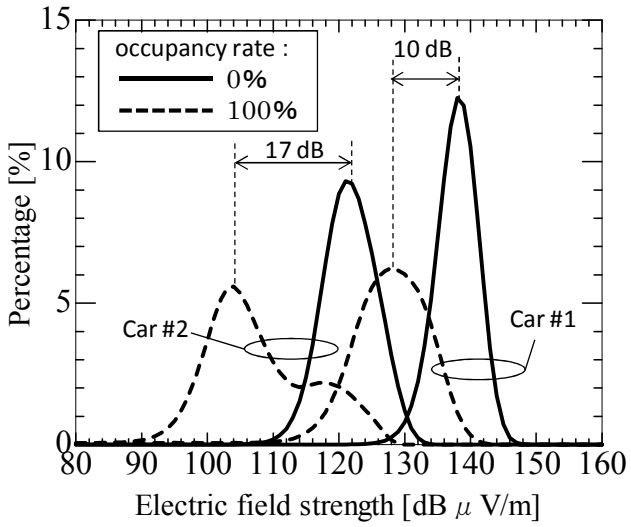

Figure 4: Electric field histograms.

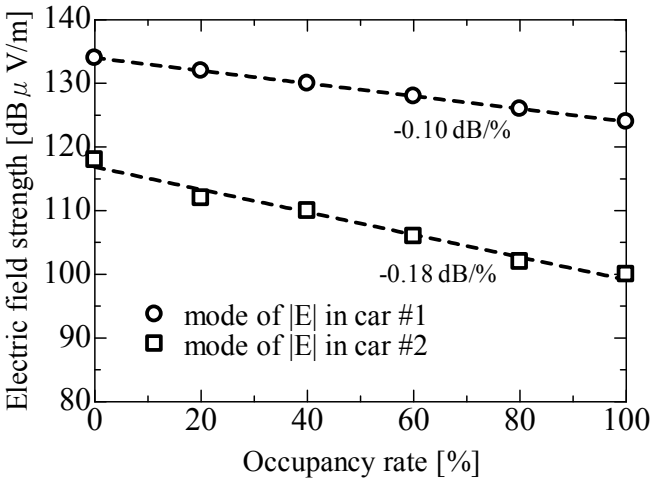

Figure 5: Attenuation characteristics versus occupancy rate.